Hindawi
Laser and Particle Beams
Volume 2022, Article ID 2836767, 7 pages
https://doi.org/10.1155/2022/2836767

Research Article

A Pulsed Synchronous Linear Accelerator for Low-Energy Proton

Yi Shen, Yi Liu, Pan Dong, Mao Ye, Huang Zhang, Liansheng Xia, Jinshui Shi, and Jianjun Deng

Institute of Fluid Physics, China Academy of Engineering Physics, P.O. Box 919-106, Mianyang 621900, China

Correspondence should be addressed to Liansheng Xia; xialiansheng@caep.cn

Received 5 May 2022; Revised 5 October 2022; Accepted 19 October 2022; Published 9 November 2022

Academic Editor: Daniele Margarone

A low-energy proton accelerator named pulsed synchronous linear accelerator (PSLA) is proposed and developed at the *Institute of Fluid Physics*, which is driven by unipolar-pulsed high voltages. Pulsed-accelerating electric fields and low-energy ion beams are precisely synchronized on temporal and spatial positions for continuous acceleration. The operating mode and the features of the PSLA are introduced. At present, the feasibility of a low-energy proton PSLA has been verified in principle. An average accelerating gradient up to 3 MV/m for protons is achieved.

1. Introduction

Low-energy proton and heavy ion with energies ranging from hundreds of keV/u to MeV/u have a wide range of applications, such as material analysis [1–3], low-energy nuclear physics [4, 5], biomedicine [6, 7], ion implanters [8], and injectors of the high-energy ion accelerator [9]. Since energy is very low, space charge effects are very strong. Especially for the acceleration of superheavy ions [10] and charged cluster particles [11] with a large mass-to-charge ratio, acceleration efficiency is very low.

The simplest way to accelerate low-energy ions is using high-voltage gaps such as that in electrostatic accelerators. However, due to insulation limits, the average acceleration gradient is about 1 ~ 2 MV/m [12], and the final achievable energy is not high. In early days and even today, great efforts have been made to build such bulky devices, such as commercially available Singleton and Tandetron produced by High Voltage Engineering Europa B. V. [13] and electrostatic Pelletron and tandem accelerators produced by National Electrostatics Corp. [14]. The radio frequency quadrupole (RFQ), which provides beam acceleration, transverse focusing, and longitudinal bunching at the same time, turns out to be a very efficient solution to boost beam energy to the MeV level, making it almost the default choice as an injector for many high-energy ion accelerators [15–17]. However, the average acceleration gradient of the RFQ is usually less than 1 MV/m. For example, the average acceleration gradient of the RFQ for the European Spallation Source is about 0.8 MV/m [18], and the whole RF system coming with the RFQ accelerator still takes a large space [19]. Moreover, usually RFQs are designed to accelerate ion beams of the specific charge-to-mass ratio. Pulsed high voltage can be used to accelerate low-energy ions, but few are built. For example, pulsed high voltage can be produced by using a Marx generator to extract the heavy ion beam [20] or by integrating the switching power supply and induction cavity to accelerate heavy ions with different mass-to-charge ratios as that in the induction synchrotron [21–23]. As far as we know, this type of accelerator does not exist, for heavy ion acceleration is still in operation at the moment. Figure 1 shows that charged particles are accelerated by three kinds of electric fields.

Based on growing needs for low-energy protons and ion accelerators, and the pursuit for compactness and cost-effectiveness, we proposed a low-energy proton accelerator driven by pulsed high voltage, namely, the pulsed synchronous linear accelerator (PSLA) [24]. Pulsed-accelerating electric fields and low-energy ion beams are precisely synchronized on temporal and spatial positions for continuous acceleration.

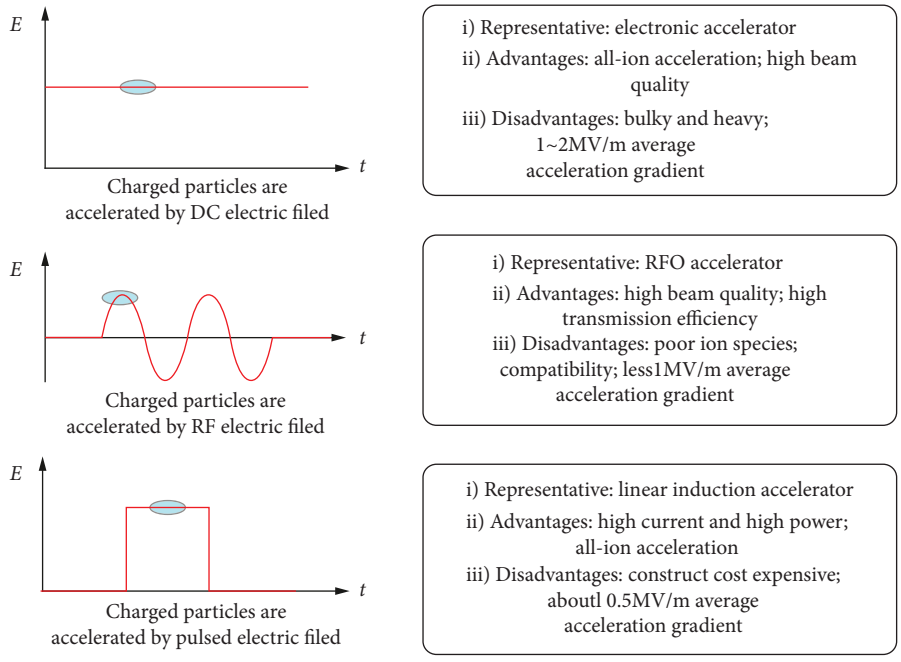

Figure 1: Charged particles are accelerated by three kinds of electric fields, their typical representatives and their advantages and disadvantages.

2. Concept of PSLA

The pulsed ion beam is accelerated in a structure consisting of many small 'cavities,' and pulsed high voltage is generated at the gaps in such a cavity. Synchronization between the pulsed high voltage and the beam is realized by controlling trigger delays for each pulse to make sure that the pulse is ready when the beam passes through the gap. To the beam itself, the PSLA is similar to a DC high-voltage accelerator, which could accelerate ions of arbitrary mass-to-charge ratios regardless of the initial velocity, including high-charge state heavy ions and cluster ions. For the insulator, the pulsed high-voltage breakdown strength is significantly improved comparing for the DC high-voltage breakdown strength. Breakdown studies indicate that insulation material can withstand field gradients of a few GV/m if the duration of pulse duration is kept to a few nanoseconds or sub-nanoseconds [25, 26]. Thus, the PSLA is easy to achieve the average acceleration gradient above 10 MV/m.

The PLSA may sound similar to virtual traveling wave acceleration in the dielectric wall accelerator [27, 28]. However, there is a significant difference: the circuit topology and parasitic parameters of the dielectric wall accelerator will cause so-called circuit coupling effects and cavity coupling effects in the dielectric wall accelerator [29]. Based on our previous study experience of the dielectric wall accelerator, we can rearrange the isolated magnetic cores on the axis and radial directions to decouple the circuit coupling and optimize the cavity structure and the matching resistance to decouple the cavity coupling. Then, our original dielectric wall accelerator [30] developed at the *Institute of Fluid Physics* (*IFP*) has gradually evolved into the present PSLA.

Figure 2 shows a schematic diagram of a simple PSLA, consisting of an ion source and ten accelerating cavities. We suppose that the beam travels through the structure, and its position is shown in Figures 2(a)–2(c), respectively. At the same time, we need to trigger accelerating pulses to synchronize with the beam motion as indicated in the same figure. The red area indicates the accelerating pulsed high voltage, while the blue area indicates the decelerating field coupled by the pulsed high voltage. The length of each area can be adjusted on demand to accommodate beam parameters like beam length and energy.

3. Numerical Simulation

3.1. [1] Proton Acceleration by Square-Pulsed High Voltage. We simulated the acceleration of a proton beam in a PSLA using the Magic software, assuming the square waveform for the pulsed high voltage, as shown in Figure 3. The beam is extracted at 50 keV and then accelerated in each acceleration cavity with a pulsed high voltage of 100 kV, and the pulse width is around 10 ~ 12 ns. The trajectory and energy distribution are shown in the same figure. When the beam is still in the structure, the head gets more energy as it passes through more cavities. As the beam leaves the structure, the main part of the beam gets the same energy. However, the head and tail have different energies due to the longitudinal space charge. The longitudinal space charge depends on the current intensity variation, so the energy modulation will be observed only in the head and tail regions where the current intensity profile dramatically changes. In addition, small transverse size of the beam suggests that transverse focusing is good enough in this case. In comparison, due to the lack of longitudinal focusing, the bunch length becomes longer due to the energy spread and longitudinal space charge.

https://doi.org/10.1155/2022/2836767

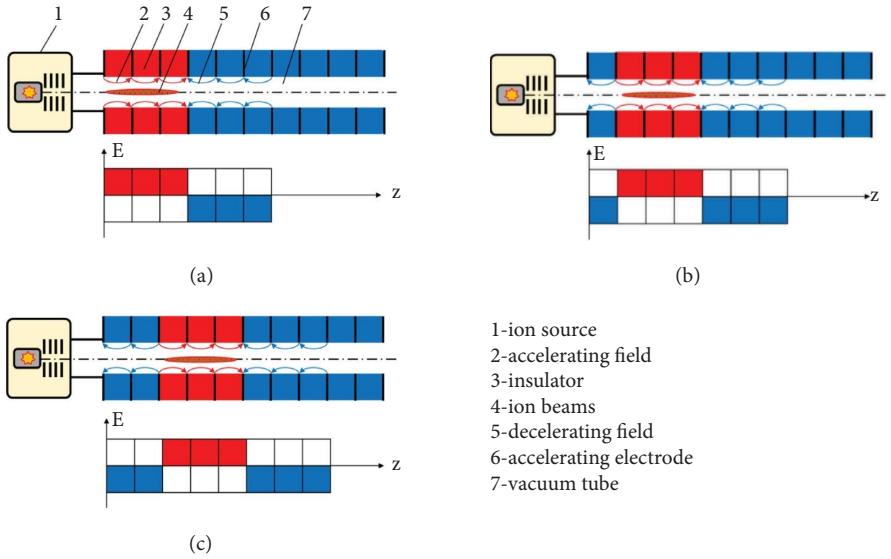

FIGURE 2: The schematic diagram of the acceleration principle of the PSLA, which includes an ion source and ten-pulsed synchronous acceleration units. (a), (b), and (c), respectively, show the situation that the position of ion beams synchronized with the pulsed electric field at time t_1, t_2, and t_3. The red area indicates the accelerating field area, and the blue area indicates the decelerating field area. The spatial length of the ion beam is about length of three acceleration structures in the axial direction. (a) $t = t_1$. (b) $t = t_2$. (c) $t = t_3$.

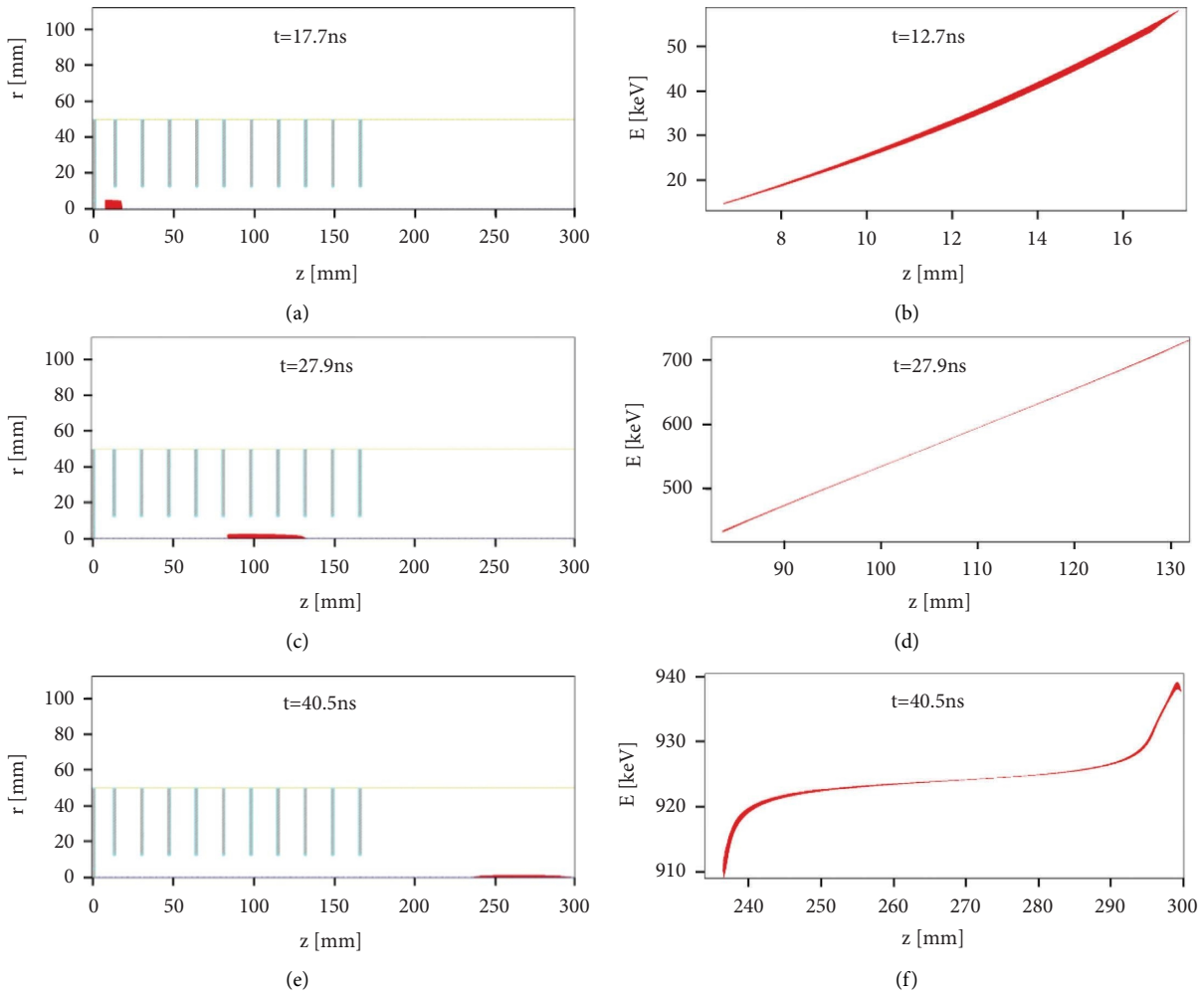

FIGURE 3: The proton beam trajectory and beam energy distribution under the 9-stage standard square waveform-pulsed high voltage.

https://doi.org/10.1155/2022/2836767

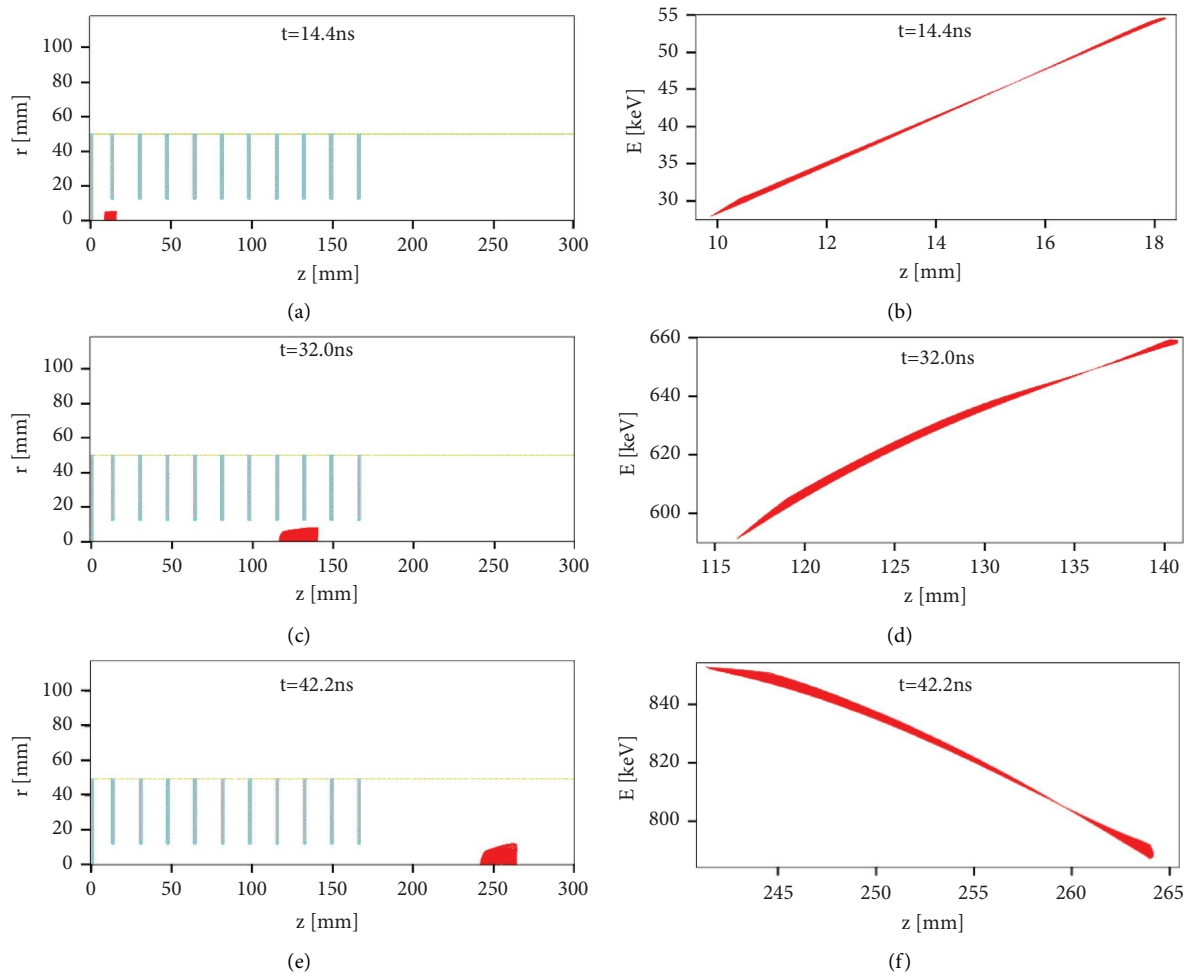

FIGURE 4: The proton beam trajectory and beam energy distribution under the 9-stage sinusoidal waveform-pulsed high voltages at another time sequence.

3.2. [2] Proton Acceleration by the Sinusoidal-Pulsed Electric Field. In order to add longitudinal focusing, a pulse shape with the rise time and fall time is similar to that of the resonant structure with a radio frequency (RF)-accelerating field. The results in Figure 4 indicate that the beam is well compressed in the longitudinal direction. In fact, actual pulsed high-voltage generated by the power source has a narrow pulse width, making it more close to the RF wave instead of a square wave.

Compared with Figure 3, the envelope of proton beams especially in the drifting tube becomes significantly bigger than that, but the total energy of the beam is lower, which is similar to the off-crest acceleration in a conventional RF structure. In order to focus the beam in the longitudinal direction, the beam head should obtain less energy and the bunch tail should gain more energy. Thus, when the beam leaves the structure, the bunch head has lower energy than the bunch tail. One can also notice that sliced energy spread is larger than that in Figure 3 in this case. In conventional RF acceleration, longitudinal focusing can be adjusted by changing the so-called synchronous phase and also the amplitude. In the case of the PSLA, one can change pulse delays and also the amplitude to form more flexible longitudinal tuning. The beam length is much shorter than that in Figure 3, which means that longitudinal focusing is working as expected. That is to say that the beam energy distribution, the beam envelope, and the length of the bunch could be adjusted by changing the time sequence for establishing the electric field of each acceleration cavity. By comparing the max energy of the bunch head and bunch tail shown in Figures 4(d) and 4(f), the max energy values of the bunch head and the bunch tail are reversed, which means that there is a suitable position for installing the target in the drift tube between $z = 180$ mm and $z = 250$ mm, where the energy of all pulsed proton beams is nearly equal. This indicates that the energy distribution of the pulsed proton beam is most optimal.

4. Experimental Verification

A prototype of the PSLA has been made, and now, it is under test. The PSLA prototype consists of a 40 keV ECR proton ion source as injector five-pulsed synchronous acceleration units and a proton beam measurement system. Each pulsed synchronous acceleration unit consisting of an acceleration cavity is driven by a pulsed power generator [31], which is

https://doi.org/10.1155/2022/2836767

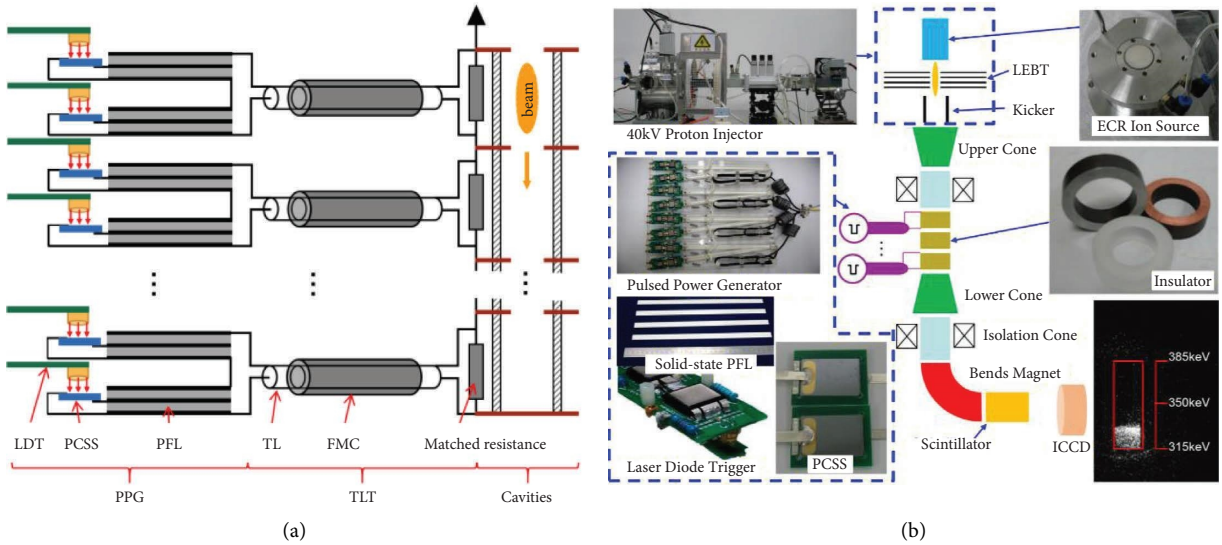

FIGURE 5: Schematic diagram and layout of the PSLA prototype. The PSLA prototype consists of a 40 keV ECR proton injector, five-pulsed synchronous acceleration units, and a proton beam measurement system. The pulsed power generator (PPG) comprises the solid-state pulse forming line (PFL), photoconductive semiconductor switch (PCSS), laser diode trigger (LDT), and transmission line transformer (TLT) composed of the ferrite magnetic ring (FMC) and transmission line (TL).

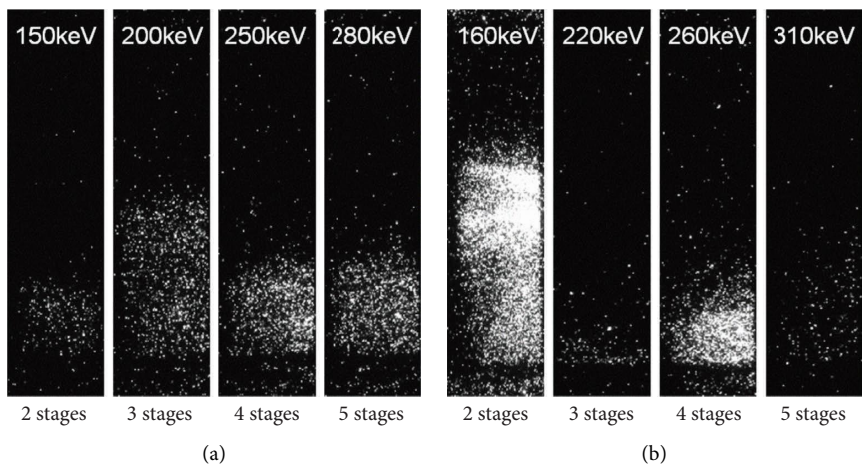

FIGURE 6: Experimental results of the proton beam energy of two-type acceleration structures of the PSLA. (a) Drifting tube structure. (b) Insulation membrane structure.

integrated by solid-state pulse forming lines, photoconductive semiconductor switches, laser diode triggers, and transmission line transformers composed of ferrite magnetic rings and transmission lines. Five accelerating cavities are serially connected. Each accelerating cavity is equivalent to a planar capacitor. Thus, the equivalent circuit of such a cavity and its driver is a transmission line transformer in topology. Each pulsed power generator supplies pulsed high voltage to the accelerating cavity with a typical amplitude of 50 ~ 80 kV, a duration of 10 ns (FWHM), and a rise time and fall time of 5 ~ 8 ns. The layout of the PSLA prototype is shown in Figure 5. The verification experiments were completed by utilizing two types of accelerating structures, which have been discussed in [24]. A proton beam measurement system consisting of a magnetic analyzer, a scintillator, and a fast ICCD camera has been built to measure beam energy.

The experimental results are shown in Figure 6. The pictures from left to right in Figures 6(a) and 6(b) show the experimental results using 2-stage to 5-stage-pulsed synchronous accelerating cavities, respectively. Here, the stage means the number of added cavities. We observed that the beam is accelerated by these synchronous-pulsed high voltages. It should be emphasized that there are differences between the conditions of the verification experiments and the simulation results, such as the operating voltage of the single acceleration unit and the number of acceleration stages. Due to the low stability and reliability of the PLSA prototype caused by the limitation of the PCSS lifetime [32], pulsed proton acceleration has not been achieved under 9-

https://doi.org/10.1155/2022/2836767

stage-pulsed high voltage with 100 kV per stage. We have only verified the results of accelerated pulsed protons at an accelerating voltage of 50 kV per stage. The experiments of proton beam acceleration of 1–5 stages have been completed, and proton beams are accelerated to a maximum energy of about 300 keV by 5-stage-pulsed synchronous acceleration units. As a result, obtained energy by adding each additional cavity is different, ranging from 30 keV to 60 keV. We expect to include more cavities in a single structure and provide 100 kV for each cavity. Figure 6 also indicates that the insulation membrane structure provides higher voltage than the drifting tube structure in our test. The total structure length is less than 10 cm in both cases, and the estimated average acceleration gradient is up to 3 MV/m.

5. Conclusion

A low-energy proton PSLA driven by pulsed high voltages is built and tested. The basic idea is that pulsed accelerating electric fields and beams can be precisely synchronized on temporal and spatial positions for continuous acceleration. In this paper, the operating mode of the PSLA is introduced, and some features of the PSLA have been discussed. The acceleration and transport of the low-energy proton beam in a PSLA have been verified in simulation and experimental verification. Our results show that an average accelerating gradient up to 3 MV/m can be obtained in the present prototype, and furthermore, future improvement can be made to increase the gradient.

Data Availability

The data used to support the findings of this study are available from the corresponding author upon reasonable request.

Conflicts of Interest

The authors declare that they have no conflicts of interest.

Acknowledgments

The authors would like to thank the associate professor Xingguang Liu, from the China Spallation Neutron Source Institute of High Energy Physics, China Academy of Science, for his assistance in polishing up this paper. This research was supported by the National Natural Science Foundation of China (Grant nos. 51977200, 12175214, and 11735012).

References

[1] T. Trivedi, S. P. Patel, P. Chandra, and P. K. Bajpai, "Ion beam facilities at the national centre for accelerator based research using a 3 MV Pelletron accelerator," *Physics Procedia*, vol. 90, pp. 100–106, 2017.

[2] M. Noun, M. Roumie, and T. Calligaro, "On the characterization of the "Paris" meteorite using PIXE, RBS and micro-PIXE," *Nuclear Instruments & Methods in Physics Research, Section B*, vol. 306, pp. 261–264, 2013.

[3] S. Matsuyama, "The microbeam system at Tohoku University," *International Journal of PIXE*, vol. 25, no. 04, pp. 153–185, 2015.

[4] G. Zhang, Y. M. Gledenov, G. Khuukhenkhuu et al., "2011 (n, α)146^{Nd} cross sections in the MeV region," *Physical Review Letters*, vol. 107, no. 25, p. 252502, Article ID 252502, 2011.

[5] J. M. Hall, B. Rusnak, and P. J. Fitsos, "High-energy neutron imaging development at LLNL," *Proceeding of 8th World Conference on Neutron Radiography*, Report number UCRL-CONF-230835, 2006.

[6] A. J. Kreiner, M. Baldo, J. R. Bergueiro et al., "Accelerator-based BNCT," *Applied Radiation and Isotopes*, vol. 88, pp. 185–189, 2014.

[7] E. Forton, F. Stichelbaut, A. Cambriani, W. Kleeven, J. Ahlback, and Y. Jongen, "Overview of the IBA accelerator-based BNCT system," *Applied Radiation and Isotopes*, vol. 67, no. 7-8, pp. S262–S265, 2009.

[8] M. Tanjo and M. Naito, "History of ion implanter and its future perspective," *SEI Technical Review*, vol. 73, pp. 22–30, 2011.

[9] B. Koubek, C. Rossi, M. Timmins, A. Grudiev, and Y. Cuvet, *Tuning of the CERN 750MHz RFQ Medical Applications*, , pp. 763–766, Proceeding of LINAC, 2016.

[10] Z. J. Wang, Y. He, A. A. Kolomiets et al., "A new compact structure for a high intensity low energy heavy-ion accelerator," *Chinese Physics C*, vol. 37, no. 12, p. 127001, Article ID 127001, 2013.

[11] T. Seki, J. Matsuo, and G. H. Takaoka, "Development of the large current cluster ion beam technology," *Proceedings of the 14th International Conference on Ion Implantation Technology*, pp. 673–676, 2002.

[12] R. Hajima, E. J. Minehara, and R. Nagai, "A full-DC injector for an energy-recovery linac," *Nuclear Instruments and Methods in Physics Research Section A: Accelerators, Spectrometers, Detectors and Associated Equipment*, vol. 528, no. 1-2, pp. 340–344, 2004.

[13] https://www.highvolteng.com/Ion_Accelerator_Systems_en.html.

[14] https://www.pelletron.com/product-category/accelerator-systems.

[15] Z. S. Li, X. J. Yin, H. Du et al., "The IH-RFQ for HIRFL-CSR injector," *Nuclear Science and Techniques*, vol. 29, no. 6, p. 89, 2018.

[16] S. Ikeda, M. Okamura, and N. Hayashizaki, "Development of four-beam IH-RFQ linear accelerator," *Nuclear Instruments and Methods in Physics Research Section B: Beam Interactions with Materials and Atoms*, vol. 462, pp. 139–142, 2020.

[17] P. N. Ostroumov, A. A. Kolomiets, S. Sharma, N. E. Vinogradov, and G. P. Zinkann, "An innovative concept for acceleration of low-energy low-charge-state heavy-ion beams," *Nuclear Instruments and Methods in Physics Research Section A: Accelerators, Spectrometers, Detectors and Associated Equipment*, vol. 547, no. 2-3, pp. 259–269, 2005.

[18] R. Garoby, A. Vergara, H. Danared et al., "Corrigendum: the European spallation source design," *Physica Scripta*, vol. 93, no. 12, p. 129501, Article ID 014001, 2018.

[19] W. Zhou, L. Rong, and J. Li, "High voltage power supply and solid state modulator for CSNS linac triode-type klystron," *2014 IEEE International Power Modulators and High Voltage Conference*, pp. 304–307, 2014.

[20] F. M. Bieniosek, E. Henestroza, and J. W. Kwan, "Performance of the K+ ion diode in the 2 MV injector for heavy ion fusion," *Review of Scientific Instruments*, vol. 73, no. 2, pp. 1042–1044, 2002.

[21] K. Takayama, Y. Arakida, T. Iwashita, Y. Shimosaki, T. Dixit, and K. Torikai, "All-ion accelerators: an injector-free synchrotron," *Journal of Applied Physics*, vol. 101, no. 6, p. 063304, Article ID 063304, 2007.

[22] T. Yoshimoto, M. Barata, T. Iwashita et al., "Heavy ion beam acceleration in the KEK digital accelerator: induction acceleration from 200 keV to a few tens of MeV," *Nuclear Instruments and Methods in Physics Research Section A: Accelerators, Spectrometers, Detectors and Associated Equipment*, vol. 733, pp. 141–146, 2014.

[23] X. Liu, T. Yoshimoto, K. Takayama et al., "Injection and induction acceleration of Ar3+ in the KEK digital accelerator," *Laser and Particle Beams*, vol. 33, no. 2, pp. 237–243, 2015.

[24] Y. Shen, Y. Liu, M. Ye et al., "Coupling and decoupling of the accelerating units for pulsed synchronous linear accelerator," *Review of Scientific Instruments*, vol. 88, no. 12, Article ID 124701, 2017.

[25] G. A. Mesyats and D. I. Proskurovsky, *Pulsed Electrical Discharge in Vacuum*, Springer-Verlag, Berlin, Germany, 1989.

[26] S. Brussaard and D. Vyuga, "A 2.5-MV subnanosecond pulser with laser-triggered spark gap for the generation of high-brightness electron bunches," *IEEE Transactions on Plasma Science*, vol. 32, no. 5, pp. 1993–1997, 2004.

[27] G. J. Caporaso, Yu-J. Chen, S. Nelson, J. Sullivan, and S. A. Hawkins, *Virtual Gap Dielectric Wall Accelerator*, 2013.

[28] G. J. Caporaso, Yu-J. Chen, and S. E. Sampayan, "The dielectric wall accelerator," *Reviews of Accelerator Science and Technology*, vol. 02, no. 01, pp. 253–263, 2009.

[29] Y. Shen, H. Zhang, and Y. Liu, "Circuit coupling and decoupling between accelerating units of dielectric wall linear accelerator," *High Power Laser and Particle Beams*, vol. 28, no. 4, Article ID 045003, 2016.

[30] L. Zhang, L. Xia, and Y. Shen, "Technologies of dielectric wall accelerator," *High Voltage Engineering*, vol. 41, no. 6, pp. 1769–1775, 2015.

[31] Y. Shen, W. Wang, Y. Liu et al., "A compact 300 kV solid-state high-voltage nanosecond generator for dielectric wall accelerator," *Review of Scientific Instruments*, vol. 86, no. 5, p. 055110, Article ID 055110, 2015.

[32] Y. Shen, Y. Liu, W. Wang, M. Ye, H. Zhang, and L. Xia, "Anode failure mechanism of GaAs photoconductive semiconductor switch triggered by laser diode," *IEEE Transactions on Plasma Science*, vol. 47, no. 10, pp. 4584–4587, 2019.